# Lifetimes and collectivity of low-lying states in $^{115}$Sn

Yu. N. Lobach,[1] L. Käubler,[2] R. Schwengner,[2] and A. A. Pasternak[3]
[1]*Institute for Nuclear Research of the Ukrainian Academy of Sciences, pr. Nauki 47, 252028 Kiev, Ukraine*
[2]*Institute of Nuclear and Hadron Physics, Research Center Rossendorf, Postfach 510119, D-01314 Dresden, Germany*
[3]*Cyclotron Laboratory, A. F. Ioffe Physico-Technical Institute, ul. Politechnitscheskaja 26, 194921 St. Petersburg, Russia*
(Received 18 August 1998)

The lifetimes of excited states in $^{115}$Sn have been measured using the Doppler shift attenuation method in the reaction $^{113}$Cd$(\alpha,2n\gamma)$ at $E_\alpha=27.2$ MeV. Lifetimes were obtained for 18 states and lifetime limits for 6 states with $E_x\leqslant 4$ MeV and $J\leqslant 23/2$. The experimentally obtained $B(\sigma L)$ values for transitions deexciting positive-parity states are compared with calculations in the framework of the Bardeen-Cooper-Schrieffer quasiparticle model and the interacting boson fermion model, whereas the values for transitions between negative-parity states are discussed qualitatively within a core-particle coupling picture. The value of $B(E2)=3.5(11)$ Weisskopf units (W.u.) for the transition linking the $19/2^-$ state of the intruder $\nu h_{11/2}\pi 2p2h$ band to the $15/2^-$ state of the $\nu h_{11/2}\otimes 2_1^+$ multiplet strongly supports the configuration $\nu h_{11/2}\pi(g_{9/2}^{-2}g_{7/2}^2)$ ascribed to this band. [S0556-2813(99)02904-0]

PACS number(s): 23.20.Lv, 27.60.+j, 21.10.Tg

## I. INTRODUCTION

During the last few years both odd- and even-mass tin isotopes have been studied very intensively. In these nuclei many different excitation modes have been observed and the variation of nuclear properties can be studied for a broad range of the neutron number $50\leqslant N\leqslant 82$ (see Ref. [1] and references therein). Even the low-energy states of the tin nuclei have a very complex nature. The structure of these states is characterized by the competition of spherical many-quasiparticle neutron excitations [2] and phonon contributions from the vibrational mode [3], as well as admixtures from the deformed low-lying proton two-particle–two-hole $(2p2h)$ intruder states [4]. Rotational bands based on two-particle–two-hole configurations have been observed in even-mass Sn nuclei [4–7]. The level scheme of $^{115}$Sn resulting from previous investigations of the $(p,n\gamma)$ [8,9], $(\alpha,n\gamma)$ [8], $(\alpha,2n\gamma)$ [10], and $(\alpha,5n\gamma)$ reactions [11] is given in the compilation of [12]. Recently, high-spin states in $^{115}$Sn were observed in heavy-ion-induced reactions [13,14]. In particular, a decoupled rotational band has been identified above the $19/2^-$ state at 3318.5 keV. This band is believed to be based upon the coupling of a $h_{11/2}$ neutron to the deformed intruder $2p2h$ band in $^{114}$Sn.

While substantial experimental progress has been made, a comprehensive theoretical description of the tin isotopes, including $^{115}$Sn, is still lacking. As shown in Sec. III, various models describe different aspects of the observed level schemes but even this description is in most cases not satisfying. Moreover, the comparison of calculated and experimental transition probabilities is a severe test of nuclear structure models. Until now lifetimes in $^{115}$Sn have been known only for a few low-lying states from Coulomb excitation [15]. The aim of present work is to extend the data on the lifetimes of excited states of the $^{115}$Sn nucleus by using the Doppler shift attenuation method (DSAM) and to interpret the structure of $^{115}$Sn levels in the framework of current nuclear models.

## II. EXPERIMENTAL METHODS AND RESULTS

Excited states of $^{115}$Sn were populated in the reaction $^{113}$Cd$(\alpha,2n\gamma)$ by bombarding a self-supporting $^{113}$Cd target of 11 mg/cm$^2$ thickness, enriched to 90.2%, with 27.2 MeV $\alpha$ particles from the cyclotron U-120 at the Institute for Nuclear Research, Kiev. The initial recoil velocity of 0.55% of the velocity of light was estimated from the reaction kinematics. Gamma-ray spectra were measured with a high-purity Ge detector of 40% relative efficiency and an energy resolution of 2.2 keV at $E_\gamma=1.33$ MeV. The detector was positioned at a distance of 17 cm from the target at angles $\Theta=30°$, 60°, 90°, 120°, and 150° relative to the beam direction. The spectrum measured at 90° is presented in Fig. 1.

The lifetimes $\tau$ of excited states in $^{115}$Sn were obtained from an analysis of the Doppler shifted $\gamma$-ray line shapes measured at different angles. This analysis was carried out using an updated version of the computer code SHAPE described in Ref. [16]. In the updated version [17] the multiple scattering of recoils is treated in greater detail by subdividing the trajectories into a number of separate segments. In this way, the correlation between the velocity of the recoil and multiple scattering angle could be accurately taken into account without simulating individual scattering events. The same version of the code was used for the lifetime determinations in our recent works for $^{113}$Sn [1], $^{115}$Sb [18], $^{117}$Sb [19], and $^{119}$I [20]; therefore, we give here only a brief description. The velocity distribution of the recoils was calculated by a Monte Carlo code that takes into account reactions at different depths of the target and the kinematics of the reaction, as well as the slowing down and deflection of the recoils. The lifetime value which gives the best fit to the experimentally obtained line shapes was accepted to be the lifetime of the state of interest. The slowing-down process was described in the code by the expression $d\varepsilon/d\rho=f_e k\varepsilon^{1/2}+f_n\varepsilon^{1/2}/(0.67\varphi_n+2.07\varepsilon)$, where $\varepsilon$ and $\rho$ are the energy and range in Lindhard's units, $k$ is the electronic Lindhard's stopping power coefficient, $f_e$ and $f_n$ are the cor-

 

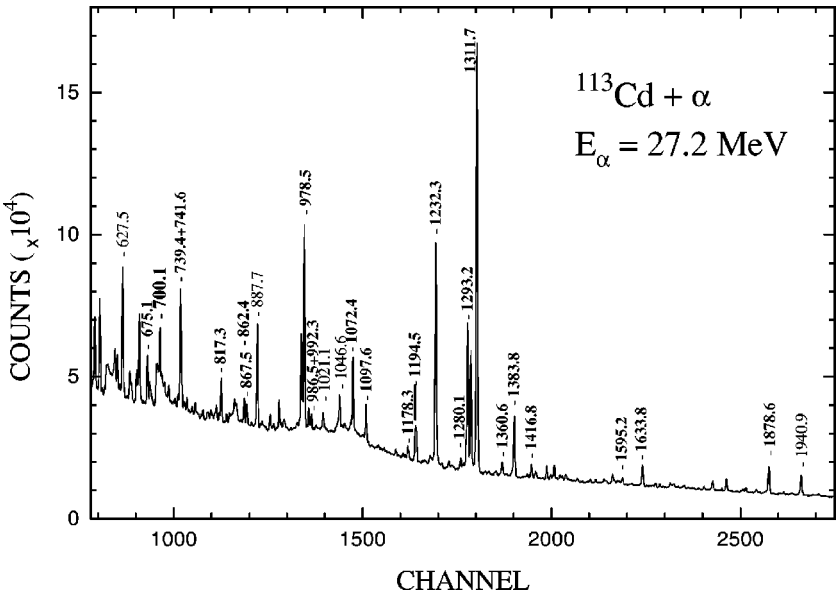


FIG. 1. $\gamma$ spectrum from $^{113}$Cd($\alpha$,2n$\gamma$) reaction at $E_\alpha = 27.2$ MeV measured at 90°. The energies of transitions used for lifetime determination in the present work marked as bold.

rection factors for the Lindhard's cross sections [21] for the electronic and nuclear stopping power, respectively, and $\varphi_n$ is an additional correction factor which characterizes the difference of the shape for the nuclear stopping power from Lindhand-Scharff-Schiott (LSS) theory [16]. When $\varphi_n = 1$, this expression approximates the shape with an accuracy better than 5% in the energy range $10 > \varepsilon^{1/2} > 0.3$, but for smaller $\varepsilon^{1/2}$ gives values that are low in comparison with LSS theory. The correction factors for the stopping process of Cd ions in the Cd target were measured in Ref. [22] using the line shape analysis from Coulomb excitation under condition $f_n = \varphi_n$. The results were the following: $f_e = 1.27 \pm 0.10$ and $f_n = \varphi_n = 0.62 \pm 0.06$. Owing to the high initial velocity of recoils in this experiment the $\varepsilon^{1/2}$ value was much greater than 1 in the large part of its range; therefore the nuclear stopping power was much lower than the electronic one. The same method for the correction factor determination was used for the reaction with heavy ions [20]. On the basis of a reliable determination of the electronic correction factor ($f_e = 1.27$), the nuclear correction factors were estimated as (a) $f_n = 0.77 \pm 0.07$, $\varphi_n = 1$, and (b) $f_n = \varphi_n = 0.70 \pm 0.07$. Both sets of factors do not contradict each other and agree with previous ones. However, the initial velocity of the recoils from the ($\alpha$,2n) reaction is 2–4 times lower than from the heavy-ion reaction. For a $\tau$ value greater than 1 ps (i.e., $\tau > \tau_{s.p.} \approx 0.3$–$0.4$ ps, where $\tau_{s.p.}$ is the characteristic time for the stopping of recoils) the main part of recoils is in the range $\varepsilon^{1/2} < 0.3$–$0.4$ where the nuclear stopping power is larger than the electronic one. To adequately account for the nuclear stopping power under such experimental conditions, it is necessary to use a slightly increased value of $f_n$ in comparison with the heavy-ion reaction. Because direct experimental measurements of the correction factors for this reaction were not performed (this is a separate and difficult experimental task) and the nuclear stopping power is comparable with the electronic one, we suggested $f_n = 0.90 \pm 0.15$ and $f_e = 1.3 \pm 0.1$. The influence of the correction factor uncertainty on the error of the $\tau$ value depends on the $\tau$ value and lies in the range 10–20 % of the $\tau$ value.

For the evaluation of the lifetime $\tau$ of a state, the time characteristics of transitions which feed this level have to be considered. In the present analysis, complex feeding patterns with up to five direct and cascade feeding components could be handled. The cascade population of the level under study was taken into account according to the decay scheme from the ($\alpha$,2n$\gamma$) reaction given in Ref. [10] which is shown in Fig. 2. The correct account of sidefeeding time ($\tau_{s.f.}$) is a difficult problem of the DSAM. Nevertheless, for many cases when the angular momenta of the entry states are not

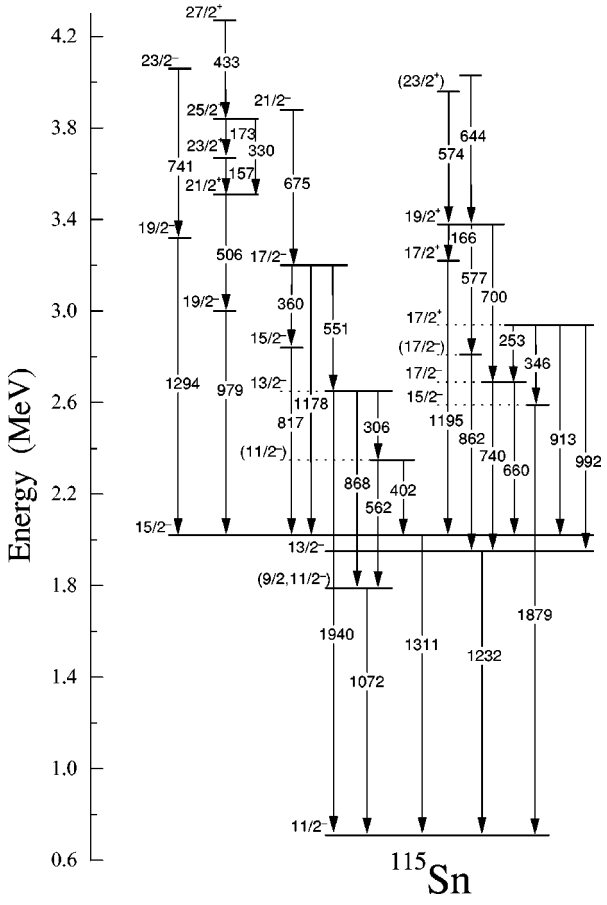


FIG. 2. Partial level scheme of $^{115}$Sn for negative-parity states (taken from Ref. [10]).

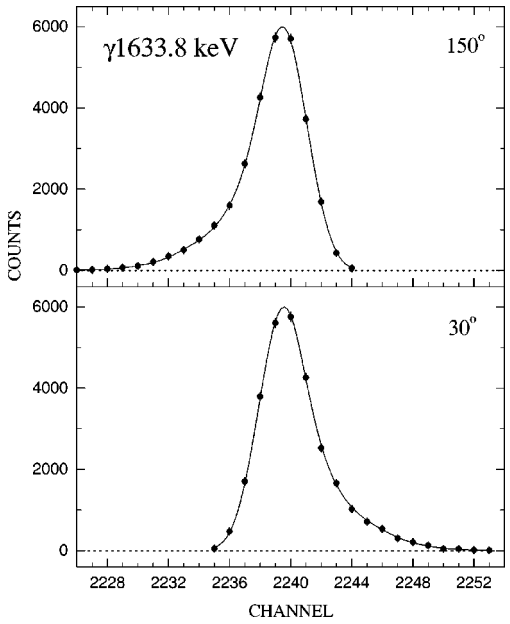


FIG. 3. Experimentally observed (dots) $\gamma$-ray line shapes for the 1633.8 keV transition measured at the angles $\theta = 30°$ and 150° and the result of the line shape analysis (the curves correspond to the best fit). The counts are normalized to equal peak areas.

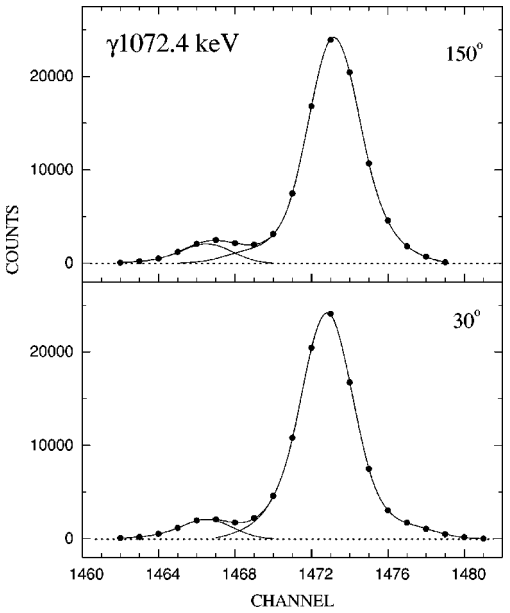


FIG. 4. As for Fig. 3, but for the 1072.4 keV transition. For the background peak at 1067.7 keV, a long lifetime was assumed, because it does not show a Doppler effect.

much different from the spins of the investigated states, the mechanism of sidefeeding is determined mainly by statistical dipole transitions and the influence of the stretch cascade is negligible. The estimations of $\tau_{\text{s.f.}}$ as well as a few experimental results give $\tau_{\text{s.f.}} \approx k_{\text{s.f.}}(E_x - E_{\text{lev}})$, where $k_{\text{s.f.}} \approx 0.01$–$0.02$ ps/MeV is more typical for light nuclei ($A \leqslant 60$) and $k_{\text{s.f.}} \approx 0.02$–$0.03$ ps/MeV for heavier nuclei [23–25]. In the present work, the value $k_{\text{s.f.}} = 0.03$ ps/MeV was adopted and this value agrees with the recent experimental result for $^{119}$I [20]. The center of the entry region has been estimated as $E_x - E_{\text{lev}} \approx 2$–$4$ MeV. Because $\tau_{\text{s.f.}} \approx 0.1$ ps $< \tau_{\text{s.p.}} \approx 0.3$–$0.4$ ps and the measured $\tau$ values exceed 1 ps in the majority of cases, one can see that the influence of $\tau_{\text{s.f.}}$ on the final $\tau$ value is rather small. Some uncertainty of $\tau_{\text{s.f.}}$ (about 10–20 %) was included in the error of $\tau$ values presented in Table I.

As an illustration, in Figs. 3 and 4, the experimental line shapes of two $\gamma$ rays measured at different angles are shown together with the result of the line shape analysis. In the analysis, the $\chi^2$ criterion was determined by varying the $\tau$ value separately for each angle. Then the $\chi^2$ values were averaged and normalized to one unit, giving the $\chi^2$ adopted value for all angles. The statistical error of lifetime was determined from the value of $\chi^2_{\min} + \Delta\chi^2$, where $\Delta\chi^2 = \chi^2_{\min}/(nN-k)$, $n$ is the number of angles used for lifetime determination, $N$ is the number of channels in the peak, and $k$ is the number of varying parameters in the analysis ($k = 2$–$5$). The lifetime values obtained in the present experiment are given in Table I. The errors include statistical errors and an uncertainty of the correction factors for electronic and nuclear stoppings.

On the basis of the measured $\tau$ values, the reduced transition probabilities $B(\sigma L)$ were calculated and presented in Table I as well. The spin and parity assignments for the levels in $^{115}$Sn were chosen according to Ref. [14]. The branching ratios of $\gamma$ transitions used in the calculations were taken from Refs. [10,12,14]. The known multipole mixing ratios $\delta$ for mixed $M1/E2$ transitions were taken from Refs. [10,12]. Unfortunately, there are some transitions with unknown $\delta$. For such transitions, the probabilities were calculated assuming either pure $M1$ or $E2$ multipolarity.

## III. DISCUSSION

The low-energy level structure of $^{115}$Sn as well as other odd-mass Sn nuclei was known to be characterized by two excitation modes, the single-particle and the collective vibration about the spherical equilibrium shape; i.e., the states of $^{115}$Sn are composed of the valence neutron occupying $1g_{7/2}$, $2d_{5/2}$, $3s_{1/2}$, $2d_{3/2}$, and $1h_{11/2}$ orbitals coupled to the spherical states of $^{114}$Sn core. However, existing experimental data for $^{115}$Sn show that even the structure of the lowest states has a more complex nature. So it was found that a number of states of both positive and negative parity cannot be reproduced in the framework of the shell model and more detailed models are needed for their interpretation. Previously, excitation energies of low-lying positive and negative-parity states in $^{115}$Sn have been described by means of the following model calculations characterizing the present status of the theoretical understanding of the nuclear structure of $^{115}$Sn: number-projected BCS quasiparticle calculations [26], the chain-calculation method [27], multistep shell-model BCS calculations [28], shell-model calculations in a very restricted configuration space [29], calculations within the interacting boson fermion model (IBFM) [30], the quasiparticle phonon calculations [31], and microscopic quasiparticle-phonon model calculations [32]. The transition probabilities have been calculated only in Refs. [26] and [30]. With the exception of the $M2$ transition $11/2^-_1 \rightarrow 7/2^+_1$, no $B(\sigma L)$ values have been calculated until now for transitions from negative-parity states. Large-scale shell-model calculations for $^{115}$Sn are at present not feasible because of the very large

TABLE I. Lifetimes of excited states in $^{115}$Sn and reduced transition probabilities $B(\sigma L)$.

| $E_x$ (keV) | $J_i^\pi$ | $\tau$ (ps) | $E_\gamma$ (keV) | $J_f^\pi$ | $I_\gamma$ (%) | $\sigma L$ | $\delta$ | $B(E2)$ (W.u.) | $B(M1)$ ($10^{-3}$ W.u.) |
|---|---|---|---|---|---|---|---|---|---|
| 497.3 | $3/2^+$ | $15.9\pm2.9$[a] | 497.3 | $1/2^+$ | 100 | $M1+E2$ | 0.21(2) | $2.1\pm0.6$ | $15\pm3$ |
| 612.8 | $7/2^+$ | $(4.70\pm0.12)\times10^{6}$[a] | 115.5 | $3/2^+$ | 100 | $E2$ | | $0.130\pm0.004$ | |
| 713.4 | $11/2^-$ | $(2.29\pm0.02)\times10^{8}$[a] | 100.7 | $7/2^+$ | 100 | $M2$[g] | | | |
| 986.5 | $5/2^+$ | $>2$[c] | 373.8 | $7/2^+$ | 6.1(14) | $M1+E2$ | $-0.26(6)$ | $<4.7$ | $<12$ |
| | | | 489.3 | $3/2^+$ | 100(6) | $M1+E2$ | 0.040(23) | $<0.6$ | $<95$ |
| | | | 986.5[b] | $1/2^+$ | 37.0(8) | $E2$ | | $<3.4$ | |
| 1280.1 | $3/2^+$ | $0.9^{+0.5}_{-0.4}$[d] | 293.6 | $5/2^+$ | 3.5(5) | $M1+E2$ | $0.23^{+0.25}_{-0.16}$ | $<74$ | $40^{+38}_{-15}$ |
| | | | 668.1 | $7/2^+$ | 3.5(8) | $E2$ | | $6.2^{+6.7}_{-2.4}$ | |
| | | | 783.0 | $3/2^+$ | 9.0(8) | $M1+E2$ | $\approx0.77$ | $2.7^{+2.4}_{-1.0}$ | $3.6^{+3.3}_{-1.3}$ |
| | | | 1280.1[b] | $1/2^+$ | 100(14) | $M1+E2$ | $-2.2^{+0.5}_{-0.8}$ | $5.7^{+5.5}_{-2.2}$ | $2.6^{+2.8}_{-1.5}$ |
| 1416.8 | $5/2^+$ | $<1.4$[e] | 136.7 | $3/2^+$ | 1.7(7) | $M1+E2$ | 0.17(15) | $>400$ | $>100$ |
| | | | 430.3 | $5/2^+$ | 0.8(6) | $M1+E2$ | $\approx0.55$ | $>1.8$ | $>1.8$ |
| | | | 804.0 | $7/2^+$ | 7(1) | $(M1+E2)$ | | $>2.7$[f] | $>2.3$[f] |
| | | | 919.7 | $3/2^+$ | 25.8(10) | $M1+E2$ | $-0.17(3)$ | $>0.15$ | $>5.4$ |
| | | | 1416.8[b] | $1/2^+$ | 100(3) | $E2$ | | $>2.2$ | |
| 1633.8 | $3/2^+$ | $1.4^{+0.5}_{-0.2}$ | 1021.1 | $7/2^+$ | 11.2(12) | $E2$ | | $1.3\pm0.4$ | |
| | | | 1136.5 | $3/2^+$ | 25(6) | $(M1+E2)$ | | $1.8\pm0.7$[f] | $3.1\pm1.1$[f] |
| | | | 1633.8[b] | $1/2^+$ | 100(9) | $(M1+E2)$ | | $1.1\pm0.3$[f] | $3.8\pm1.0$[f] |
| 1785.6 | $(9/2^-)$ | $1.0^{+0.3}_{-0.2}$ | 1072.4[b] | $11/2^-$ | 100 | $(M1+E2)$ | $-1.6(2)$ | $13\pm3$ | $7.5\pm2.2$ |
| 1857.5 | $7/2^+$ | $0.5\pm0.1$ | 1360.6[b] | $3/2^+$ | 100 | $E2$ | | $10.9\pm2.2$ | |
| 1945.6 | $13/2^-$ | $1.9^{+0.6}_{-0.4}$ | 1232.3[b] | $11/2^-$ | 100 | $M1+E2$ | $12^{+5}_{-3}$ | $4.6\pm1.2$ | $0.07\pm0.05$ |
| 1996.3 | $11/2^+$ | $1.5^{+0.3}_{-0.2}$ | 1383.8[b] | $7/2^+$ | 100 | $E2$ | | $3.2\pm0.5$ | |
| 2024.8 | $15/2^-$ | $1.4^{+0.6}_{-0.4}$ | 1311.7[b] | $11/2^-$ | 100 | $E2$ | | $4.7\pm1.6$ | |
| 2084.2 | $7/2^+$ | $1.3^{+0.4}_{-0.2}$ | 804.0 | $3/2^+$ | 11(3) | $E2$ | | $2.6\pm0.7$ | |
| | | | 1097.6[b] | $5/2^+$ | 100(9) | $(M1+E2)$ | | $5.0\pm1.1$[f] | $7.9\pm1.7$[f] |
| | | | 1471.8 | $7/2^+$ | 66(6) | $(M1+E2)$ | | $0.7\pm0.2$[f] | $2.2\pm0.5$[f] |
| | | | 1586.9 | $3/2^+$ | 50(9) | $E2$ | | $0.4\pm0.1$ | |
| 2207.7 | $5/2^+$ | $1.5\pm0.5$ | 1221.1 | $5/2^+$ | 100(7) | $(M1+E2)$ | | $4.6\pm1.7$ | $8.9\pm3.3$ |
| | | | 1595.2[b] | $7/2^+$ | 53(14) | $(M1+E2)$ | | $0.7\pm0.3$[f] | $2.3\pm1.0$[f] |
| 2591.9 | $(15/2^-)$ | $>3.5$ | 1878.6[b] | $11/2^-$ | 100 | $(E2)$ | | $<0.3$ | |
| 2653.4 | $13/2^-$ | $1.7^{+2.0}_{-0.7}$ | 306.0 | $11/2^-$ | 7(2) | $(M1+E2)$ | | $229\pm147$[f] | $28\pm18$[f] |
| | | | 628.2 | $15/2^-$ | 54(5) | $(M1+E2)$ | | $44\pm26$[f] | $22\pm13$[f] |
| | | | 867.5[b] | $11/2^-$ | 100(10) | $(M1+E2)$ | | $16\pm9$[f] | $15\pm9$[f] |
| | | | 1940.0 | $11/2^-$ | 46(9) | $(M1+E2)$ | | $0.14\pm0.09$[f] | $0.7\pm0.4$[f] |
| 2685.1 | $17/2^-$ | $1.8^{+0.7}_{-0.4}$ | 660.0 | $15/2^-$ | 72(12) | $M1+E2$ | 1.9(3) | $37\pm13$ | $6.2\pm2.6$ |
| | | | 739.4[b] | $13/2^-$ | 100(12) | $E2$ | | $38\pm13$ | |
| 2807.5 | (17/2) | $0.9^{+0.5}_{-0.4}$ | 862.4[b] | $13/2^-$ | 100 | $(E2)$ | | $71\pm32$ | |
| 2842.1 | $15/2^-$ | $0.9^{+0.3}_{-0.2}$ | 496.1 | $11/2^-$ | 32(4) | $E2$ | | $200\pm62$ | |
| | | | 817.3[b] | $15/2^-$ | 100(10) | $(M1+E2)$ | | $51\pm16$[f] | $40.7\pm9.0$[f] |
| | | | 897.7 | $13/2^-$ | 22(4) | $(M1+E2)$ | | $7.1\pm2.4$[f] | $6.7\pm1.5$[f] |
| 2937.9 | $(17/2^-)$ | $>2.5$ | 252.8 | $17/2^-$ | 33(15) | $(M1+E2)$ | | $<1390$[f] | $<188$[f] |
| | | | 346.0 | $15/2^-$ | 30(15) | $(M1+E2)$ | | $<260$[f] | $<40$[f] |
| | | | 913.1 | $15/2^-$ | 100(50) | $(M1+E2)$ | | $<6.6$[f] | $<7$[f] |
| | | | 992.3[b] | $13/2^-$ | 66(33) | $(E2)$ | | $<2.9$ | |
| 3003.4 | $19/2^-$ | $0.9^{+0.5}_{-0.3}$ | 978.5[b] | $15/2^-$ | 100 | $E2$ | | $33\pm13$ | |
| 3203.2 | $17/2^-$ | $>1.5$ | 360.1 | $(15/2^-)$ | 39(3) | $(M1+E2)$ | | $<460$[f] | $<78$[f] |
| | | | 550.1 | $13/2^-$ | 100(3) | $E2$ | | $<143$ | |
| | | | 559 | $15/2^-$ | 11(2) | $(M1+E2)$ | | $<15$[f] | $<6$[f] |

TABLE I. (*Continued*).

| $E_x$ (keV) | $J_i^\pi$ | $\tau$ (ps) | $E_\gamma$ (keV) | $J_f^\pi$ | $I_\gamma$ (%) | $\sigma L$ | $\delta$ | $B(E2)$ (W.u.) | $B(M1)$ ($10^{-3}$ W.u.) |
|---|---|---|---|---|---|---|---|---|---|
| | | | 1178.3[b] | $15/2^-$ | 55(6) | $(M1+E2)$ | | $<1.7$[f] | $<3.1$[f] |
| | | | 1257.8 | $13/2^-$ | 21(3) | $E2$ | | $<0.5$ | |
| 3219.7 | $17/2^+$ | $1.8^{+0.6}_{-0.4}$ | 1194.5[b] | $15/2^-$ | 100 | $E1$[h] | | | |
| 3318.5 | $19/2^-$ | $1.9^{+0.7}_{-0.5}$ | 115.2 | $17/2^-$ | $<0.2$ | $(M1+E2)$ | | $<1200$[f] | $<20$[f] |
| | | | 475.4 | $(15/2^-)$ | 5.0(3) | $(E2)$ | | $28\pm11$ | |
| | | | 674.4 | $15/2^-$ | 3.0(5) | $E2$ | | $2.8\pm1.1$ | |
| | | | 1293.2[b] | $15/2^-$ | 100(5) | $E2$ | | $3.5\pm1.1$ | |
| 3384.7 | $(19/2^+)$ | $0.6^{+0.3}_{-0.2}$ | 165.5 | $17/2^+$ | 20.3(12) | $(M1+E2)$ | $-0.05(5)$ | $<520$ | $2000\pm800$ |
| | | | 576.6 | (17/2) | 7.3(20) | $(M1+E2)$ | | $45\pm21$[f] | $19\pm9$[f] |
| | | | 700.1[b] | $17/2^-$ | 100(5) | $(E1)$[i] | | | |
| 3878.3 | $21/2^-$ | $1.2^{+0.6}_{-0.3}$ | 560.6 | $19/2^-$ | 32(3) | $(M1+E2)$ | | $91\pm32$[f] | $37\pm13$[f] |
| | | | 675.1[b] | $17/2^-$ | 100(5) | $E2$ | | $111\pm38$ | |
| 4059.9 | $23/2^-$ | $>1.5$ | 181.0 | $21/2^-$ | 3.4(4) | $(M1+E2)$ | | $<400$[f] | $<90$[f] |
| | | | 588.2 | $19/2^-$ | 6.6(5) | $E2$ | | $<11$ | |
| | | | 741.6[b] | $19/2^-$ | 100(4) | $E2$ | | $<55$ | |
| | | | 801.4 | $(19/2^-)$ | 4.7(5) | $(E2)$ | | $<1.7$ | |
| | | | 1055.9 | $19/2^-$ | 22(1) | $E2$ | | $<2.0$ | |

[a]Reference [12].
[b]Gamma ray used for the determination of the lifetime $\tau$.
[c]Reference [12]: $\tau=2.84\pm0.14$ ps.
[d]Reference [12]: $\tau=0.63\pm0.13$ ps.
[e]Reference [12]: $\tau=0.51\pm0.06$ ps.
[f]For a pure $E2$ or $M1$ transition.
[g]$B(M2)=0.110\pm0.004$ W.u.
[h]$B(E1)=(1.3^{+1.6}_{-0.3})\times10^{-4}$ W.u.
[i]$B(E1)=(1.7\pm0.7)\times10^{-3}$ W.u.

configuration spaces required. As concluded in Ref. [1], shell-model calculations should also consider the breakup of the $Z=50$ proton core.

Most of the calculations mentioned above assume closed cores of 50 neutrons ($\nu$) and 50 protons ($\pi$). The remaining $N-50$ valence neutrons are considered to occupy the $1g_{7/2}$, $2d_{5/2}$, $3s_{1/2}$, $2d_{3/2}$, and $1h_{11/2}$ shells, but this configuration space is drastically truncated in all known calculations.

In Sec. III A, we compare the results of our lifetime measurements for positive-parity states with theoretical values available in the literature. Our measured lifetimes of negative-parity states are qualitatively discussed in Sec. III B in the framework of a core-particle coupling (CPC) picture. In Sec. III C the first case of an experimentally determined $B(E2)$ value for the transition from a state of $\nu h_{11/2}\pi 2p2h$ band in an odd-mass tin nucleus to a state out of this band is discussed.

### A. Positive-parity states

A partial level scheme of $^{115}$Sn is given in Fig. 5, showing all positive-parity states observed until now up to $E_x=1734$ keV [12]. Our measured lifetime values for the levels at 986.5 and 1280.1 keV (Table I) agree reasonably well with those determined by means of Coulomb-excitation measurements [15]. A discrepancy is found for the state at 1416.8 keV because our $\tau=1.4\pm0.3$ ps disagrees with $\tau=0.51\pm0.16$ ps from Coulomb-excitation measurements. We cannot rule out the existence of additional unknown transitions which feed the state at 1416.8 keV. Consequently, the present $\tau$ value must be regarded as an upper limit for this state.

Spectroscopic factors have been measured for the $1/2^+_1$, $3/2^+_1$, $7/2^+_1$, $11/2^-_1$, and $5/2^+_1$ states [33]. For the $11/2^-_1$ state, a $C^2S$ value near unity has been found whereas for the positive-parity states values of $C^2S<1$ have been deduced, allowing the conclusion that only the $11/2^-_1$ state is a rather pure $\nu h_{11/2}$ single-particle state.

The ground state of $^{115}$Sn is a $1/2^+$ state and therefore the lowest $3/2^+$ and $5/2^+$ states can originate from the coupling of quadrupole phonons in the core with ground state or $d_{3/2}$ and $d_{5/2}$ single-particle states. The result from Coulomb excitation in $^{117,119}$Sn [34] show that the two lowest $3/2^+$ states in these nuclei have a clearly discernible nature and they must be a good example of pure collective and single-particle states, but at the same time both $5/2^+$ states are more mixed than the $3/2^+$ ones. The results of present work, as well as Ref. [15], indicate the presence of a quadrupole component in the first two $3/2^+$ and the first two $5/2^+$ states in this nucleus. The $B(E2)$ values (Table I) for the transitions from $3/2^+$ states and from the first two $5/2^+$ states to the ground state are slightly enchanced with respect to the single-particle estimate and are closer to each other in comparison with the corresponding ones in $^{117,119}$Sn. Therefore, this must be a hint of the collective admixtures of these states.

In Table II, our experimental $B(\sigma L)$ values are compared with theoretical results obtained by number-projected BCS quasiparticle calculations [26]. In this approach, the excited states are treated as one- or three-quasiparticle neutron excitations of the $1g_{7/2}$, $2d_{5/2}$, $3s_{1/2}$, $2d_{3/2}$, and $1h_{11/2}$ shells. The energies of the levels with a large one-quasiparticle component are well reproduced by these calculations, but the

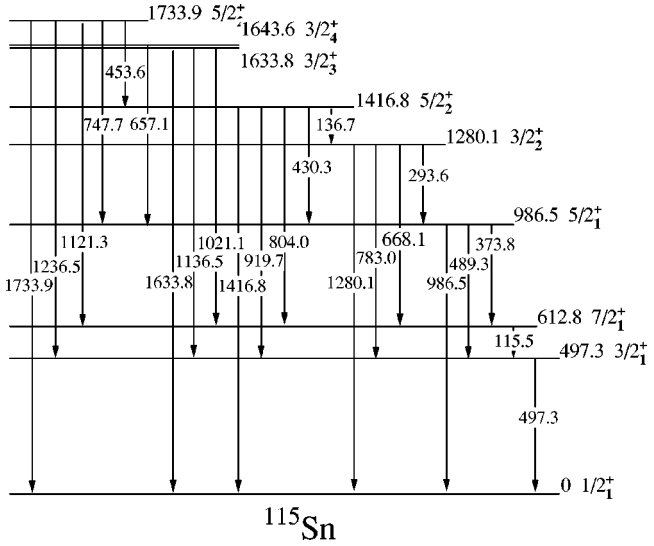


FIG. 5. The lowest positive-parity states in $^{115}$Sn (taken from Ref. [12]).

calculated levels with three-quasiparticle components come out higher than the experimental ones. The discrepancy in the excitation energies was attributed to the restricted basis. Thus, for example, the energies of the $2_1^+$ states in even-mass Sn isotopes are calculated up to 0.5 MeV higher than the experimental values. In the same calculations [26] it was also shown that electromagnetic properties are strongly dependent on the three-quasiparticle components in the wave functions. Looking at the calculated $B(E2)$ values in more detail, nearly all theoretical values are smaller than the experimental results. Most of the theoretical values have the same order of magnitude as the experimental values, but in four cases the calculated values are smaller by a factor of $10^{-2}$–$10^{-3}$. The comparison of calculated $B(M1)$ values with experimental values shows a more dramatic divergence. This divergence also allows the conclusion that experimental states include collective contributions as well as a mixing of the states which are not considered by calculations in the framework of this model.

In Table II, the results of calculations performed in the framework of the U(6)×U(20) symmetry limit of the IBFM [30] are also presented. For some transitions, the calculated $B(\sigma L)$ values are in reasonable agreement with the experimental ones. However, some observed transitions are forbidden in this model; at the same time some calculated transitions are strong although they are found to be weak in the experiment. The reason of such a divergence, as discussed in Ref. [30], must be due to adherence to the exact symmetry limit.

TABLE II. Experimental and calculated transition probabilities for low-lying positive parity states in $^{115}$Sn.

| $E_x$ (keV) | $J_i^\pi$ | $J_f^\pi$ | $E_\gamma$ (keV) | $B(M1)_{\text{expt}}$ ($10^{-3}$ W.u.) | $B(M1)_{\text{calc}}$[a] ($10^{-3}$ W.u.) | $B(E2)_{\text{expt}}$ (W.u.) | $B(E2)_{\text{calc}}$[a] (W.u.) | $B(E2)_{\text{calc}}$[b] (W.u.) |
|---|---|---|---|---|---|---|---|---|
| 497.3 | $3/2_1^+$ | $1/2_1^+$ | 497.3 | $15\pm3$[c] | 5.2 | $2.1\pm0.6$[c] | 2.8 | 2.16 |
| 612.8 | $7/2_1^+$ | $3/2_1^+$ | 115.5 | | 0.037 | $0.130\pm0.004$[c] | 0.037 | 0.42 |
| 986.5 | $5/2_1^+$ | $7/2_1^+$ | 373.8 | $<12$ | 1.2 | $<4.7$ | 0.41 | 1.0 |
| | | $3/2_1^+$ | 489.3 | $<95$ | 64 | $<0.6$ | 0.0096 | 0.25 |
| | | $1/2_1^+$ | 986.5 | | | $<3.4$ | 2.3 | |
| 1280.1 | $3/2_2^+$ | $5/2_1^+$ | 293.6 | $40^{+38}_{-15}$ | 0.068 | $<74$ | 0.024 | |
| | | $7/2_1^+$ | 668.1 | | | $6.2^{+6.7}_{-2.4}$ | 4.2 | |
| | | $3/2_1^+$ | 783.0 | $3.6^{+3.3}_{-1.3}$ | 0.32 | $2.7^{+2.4}_{-1.0}$ | 0.059 | |
| | | $1/2_1^+$ | 1280.1 | $2.6^{+2.8}_{-1.5}$ | 1.3 | $5.7^{+5.5}_{-2.2}$ | 1.7 | |
| 1416.8 | $5/2_2^+$ | $3/2_2^+$ | 136.7 | $>100$ | | $>400$ | | |
| | | $5/2_1^+$ | 430.3 | $>1.8$ | 0.87 | $>1.8$ | 0.069 | 1.78 |
| | | $7/2_1^+$ | 804.0 | $(>2.3)$[d] | $2.4\times10^{-5}$ | $(>2.7)$[d] | 4.2 | |
| | | $3/2_1^+$ | 919.7 | $>5.4$ | 17 | $>0.15$ | 0.18 | |
| | | $1/2_1^+$ | 1416.8 | | | $>2.2$ | 4.6 | 7.03 |
| 1633.8 | $3/2_3^+$ | $7/2_1^+$ | 1021.1 | | | $1.3\pm0.4$ | 0.6 | |
| | | $3/2_1^+$ | 1136.5 | $(3.1\pm1.1)$[d] | 9.5 | $(1.8\pm0.7)$[d] | 1.0 | |
| | | $1/2_1^+$ | 1633.8 | $(3.8\pm1.0)$[d] | 26 | $(1.1\pm0.3)$[d] | 0.85 | |
| 1643.6 | $3/2_4^+$ | $5/2_1^+$ | 657.1 | | 2.7 | | 1.1 | |
| 1733.9 | $5/2_3^+$ | $3/2_2^+$ | 453.6 | | | | | |
| | | $5/2_1^+$ | 747.7 | | | | 1.3 | |
| | | $7/2_1^+$ | 1121.3 | | | | 0.11 | |
| | | $3/2_1^+$ | 1236.5 | | 2.3 | | 9.2 | |
| | | $1/2_1^+$ | 1733.9 | | | | 0.47 | |

[a]Reference [26].
[b]Reference [30].
[c]Reference [12].
[d]For a pure $E2$ or $M1$ transition.

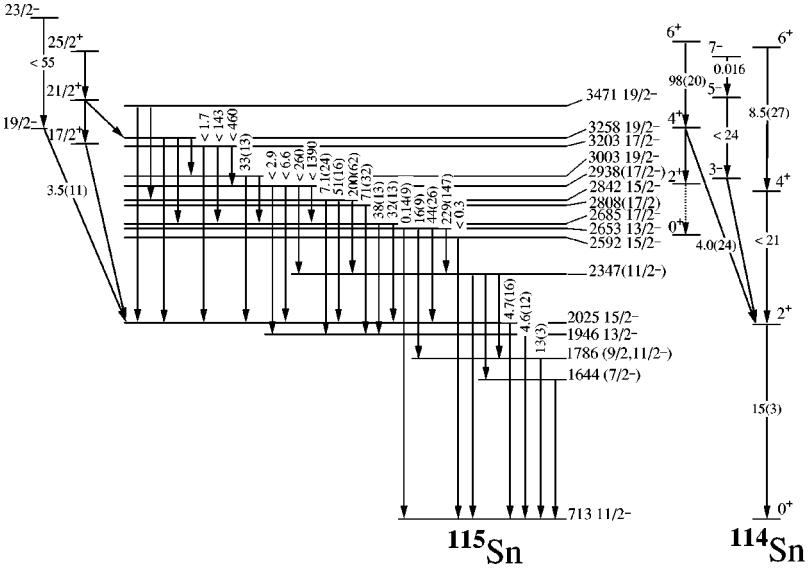


FIG. 6. Partial level scheme of $^{115}$Sn [10,14] showing states built on the $\nu h_{11/2}$ single-particle state at 713.4 keV in comparison with yrast states and some members of the $\pi 2p2h$ intruder band in $^{114}$Sn [4]. For $^{115}$Sn, labels on the arrows indicate our measured $B(E2)$ values (W.u.). The $B(E2)$ values for $^{114}$Sn are taken from Ref. [37].

Finally, one can see from Table II a very different description by both models of the same states.

### B. Negative-parity states

The low-lying negative-parity states in odd-mass Sn isotopes are interpreted as the coupling of a valence $h_{11/2}$ neutron to low-lying positive-parity states in the even-even cores [1,11,14,35]. For $^{115}$Sn, results of CPC calculations are not available. Therefore, we compare qualitatively our experimental observations in $^{115}$Sn with characteristics of a CPC picture.

In Fig. 6, partial level schemes are given, showing levels in $^{115}$Sn built on the $\nu h_{11/2}$ state at 713.4 keV, as well as the yrast states and some members of the $\pi 2p2h$ intruder band of $^{114}$Sn. Except for the 1644, 3258, and 3471 keV states, observed in a heavy-ion-induced reaction [14], all the $^{115}$Sn levels presented in Fig. 6 have been identified in our previous work [10].

According to the CPC picture, the experimentally observed $19/2^-_1$-$15/2^-_1$-$11/2^-_1$ level spacings in $^{115}$Sn should be close to the $4^+_1$-$2^+_1$-$0^+_1$ ones in $^{114}$Sn. Furthermore, we should observe five states with $7/2^- \leqslant J^\pi \leqslant 15/2^-$ arising from the multiplet $\nu h_{11/2} \otimes 2^+_1$ ($^{114}$Sn). Because of the weak coupling, such a multiplet should be degenerate; i.e., the states of the multiplet should be concentrated in a relatively narrow energy range near 2.0 MeV [$E(\nu h_{11/2}) = 0.713$ MeV$+E(2^+_1,\ ^{114}\mathrm{Sn}) = 1.300$ MeV]. Nearly all of these features of the CPC are in accordance with our experimental findings. The states at 1644 and 2347 keV in $^{115}$Sn are linked by direct transitions to the $11/2^-_1$ state at 713.4 keV. Therefore, one can suppose that they belong to the members of the $\nu h_{11/2} \otimes 2^+_1$ multiplet, too. The spin assignment for the state at 1786 keV is uncertain because different values have been given in Refs. [10] and [14]. Nevertheless, it is likely that we have observed in $^{115}$Sn the complete multiplet and therefore the assignment $(7/2^-)$ is proposed for the state at 1644 keV.

Moreover, assuming CPC, we should also observe states of the $\nu h_{11/2} \otimes 4^+_1$ multiplet and other states arising from the coupling of a $h_{11/2}$ neutron to the $^{114}$Sn core states shown in Fig. 6. Negative-parity states with 2592 keV$\leqslant E_x \leqslant$3003 keV may be considered as members of the $\nu h_{11/2} \otimes 4^+_1$ multiplet and the higher-lying $17/2^-$ and $19/2^-$ states as members of the $\nu h_{11/2} \otimes 6^+_1$ multiplet. The $17/2^+$, $21/2^+$, and $25/2^+$ states may result from a coupling of a $h_{11/2}$ neutron to the $3^-$, $5^-$ and $7^-$ core states, respectively.

In Fig. 6, the experimental $B(E2)$ values are given as well. In CPC with weak coupling, the $B(E2)$ values of the transitions from states of the $\nu h_{11/2} \otimes 2^+_1$ multiplet to the $11/2^-_1$ level in $^{115}$Sn are expected to be equal to each other and equal to the $B(E2)$ value of the $2^+_1 \rightarrow 0^+$ transition in $^{114}$Sn [36]. Only one of these transitions in $^{115}$Sn (at 1786.5 keV) has nearly the same $B(E2)$ value as the $2^+_1 \rightarrow 0^+_1$ transition in $^{114}$Sn. The reason for this might be the mixing in the $4^+_1$ and $2^+_1$ wave functions in $^{114}$Sn as found, e.g., in our shell-model calculations of $^{112}$Sn levels [1] as well as the decisive role of two-phonon components in the $4^+_1$ state [3]. Some of the experimental $B(E2)$ values of the transitions between the $\nu h_{11/2} \otimes 4^+_1$ and $\nu h_{11/2} \otimes 2^+_1$ multiplets in $^{115}$Sn

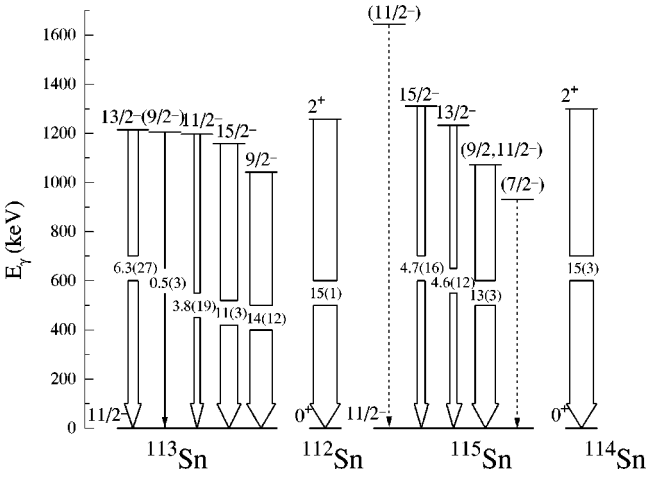


FIG. 7. Comparison of the $B(E2)$ values for the transitions from the $h_{11/2} \otimes 2^+_1$ multiplet states to the $\nu h_{11/2}$ single-particle state in $^{113}$Sn [1] and $^{115}$Sn. The energy of the $11/2^-_1$ states has been shifted to zero.

are much larger than the corresponding $B(E2,4_1^+ \rightarrow 2_1^+)$ value in $^{114}$Sn. Most of the transitions deexciting the states above 2.5 MeV are strongly enhanced, thus giving a hint at collective admixtures to these states. Such $B(E2)$ values are typical for intraband transitions of rotational bands built on three-quasiparticle states in transitional and deformed nuclei. From values of 10 Weisskopf units (W.u.)$\leqslant B(E2) \leqslant$100 W.u., a deformation of $0.05 \leqslant \beta_2 \leqslant 0.20$ can be estimated. Probably, a change from spherical to slightly deformed states appears already in this low-energy region.

In Fig. 7, the $E2$ transition probabilities from the members of the $\nu h_{11/2} \otimes 2_1^+$ multiplet to $\nu h_{11/2}$ single-particle state in $^{115}$Sn are compared with the corresponding ones in $^{113}$Sn where the members of such multiplet were identified more completely [1]. Only two $B(E2)$ values in $^{113}$Sn are nearly equal to the $B(E2,2_1^+ \rightarrow 0_1^+)$ value in $^{112}$Sn.

Summarizing, on the basis of the measured $B(E2)$ values one can conclude that the CPC picture is only an approximation to the low-lying negative-parity states in $^{113}$Sn and $^{115}$Sn.

### C. $\nu h_{11/2} \pi 2p2h$ band

Above the $19/2^-$ state at 3319 keV in $^{115}$Sn, a band was observed and discussed as a rotational band built on the configuration $\nu h_{11/2} \pi (g_{9/2}^{-2} g_{7/2}^2)$, including the deformed $\pi 2p2h$, $Z=50$ core excitation in $^{114}$Sn [13]. Assuming this interpretation, the 1293.2-keV transition (Table I) links the $19/2^-$ state of the $\nu h_{11/2} \pi (g_{9/2}^{-2} g_{7/2}^2)$ band with the $15/2^-$ state of the $\nu h_{11/2} \otimes 2_1^+$ multiplet (Fig. 6). The $11/2^-$ bandhead and the $15/2^-$ state of this band have not been observed in the experiments. The $19/2^-$ state at 3319 keV in $^{115}$Sn corresponds to the $4^+$ state at 2614 keV in $^{114}$Sn. As seen in Fig. 6, the values $B(E2,19/2^- \rightarrow 15/2^-) = 3.5 \pm 1.1$ W.u. for the transition deexciting the 3319-keV state in $^{115}$Sn and $B(E2,4^+ \rightarrow 2_1^+) = 4.0 \pm 2.4$ W.u. for the transition deexciting the 2614-keV level in $^{114}$Sn agree well. The $4^+$ state at 2614 keV in $^{114}$Sn [4] belongs to the deformed $\pi 2p2h$ intruder band. This agreement is an additional experimental argument for the interpretation of the band in $^{115}$Sn as discussed above. In our experiment, the transition probability for the transition from $\nu h_{11/2} \pi 2p2h$ band to the state out of this band in odd-mass tin nuclei has been deduced. The occurrence of such transition is also a hint at probably very small, but nevertheless important, admixtures of the $\nu h_{11/2} \pi 2p2h$ configuration to low-lying multiplet states in $^{115}$Sn.

## IV. CONCLUSIONS

The lifetimes of excited states in $^{115}$Sn have been measured using the DSAM in the reaction $^{113}$Cd$(\alpha,2n\gamma)^{115}$Sn at 27.2 MeV. As a result, lifetimes for 18 states and lifetime limits for 6 states were obtained. The analysis of the transition probabilities in $^{115}$Sn allows the following conclusions.

(i) Most of the experimentally obtained $B(E2)$ values for transitions deexciting low-lying states in $^{115}$Sn are enhanced, giving a hint at collective admixtures even in these low-lying states.

(ii) The picture of core-particle coupling is only an approximation for the observed multipletlike negative parity states in $^{115}$Sn.

(iii) In this work, the $B(E2)$ value for a transition from the $\nu h_{11/2} \pi 2p2h$ band in an odd-mass tin nucleus to a state out of this band has been determined. The agreement with the $B(E2)$ value of the corresponding transition in $^{114}$Sn confirms the proposed configuration $\nu h_{11/2} \pi (g_{9/2}^{-2} g_{7/2}^2)$ for this band in $^{115}$Sn [13] and gives a hint at small admixtures of this configuration to low-lying multiplet states in $^{115}$Sn.

## ACKNOWLEDGMENTS

The authors would like to thank S. Juutinen for helpful discussions and communication of his experimental data prior publication.

[1] L. Käubler, Yu. N. Lobach, V. V. Trishin, A. A. Pasternak, M. F. Kudojarov, H. Prade, J. Reif, R. Schwengner, G. Winter, J. Blomqvist, and J. Döring, Z. Phys. A **358**, 303 (1997).

[2] A. Van Poelgeest, J. Bron, W. H. A. Hesselink, K. Allaart, J. J. A. Zalmstra, M. J. Uitzinger, and H. Verheul, Nucl. Phys. **A346**, 70 (1980).

[3] W. Andrejtscheff, L. K. Kostov, P. Petkov, Y. Sy Savane, Ch. Stoyanov, P. von Brentano, J. Eberth, R. Reinhardt, and K. O. Zell, Nucl. Phys. **A505**, 397 (1989).

[4] J. Bron, W. H. A. Hesselink, A. van Poelgeest, J. J. A. Zalmstra, M. J. Uitzinger, H. Verheul, K. Heyde, M. Waroquier, H. Vincx, and P. van Isacker, Nucl. Phys. **A318**, 335 (1979).

[5] R. Wadsworth, H. R. Andrews, C. W. Beausang, R. M. Clark, J. DeGraaf, D. B. Fossan, A. Galindo-Uribarri, I. M. Hibbert, K. Hauschild, J. R. Hughes, V. P. Janzen, D. R. LaFosse, S. M. Mullins, E. S. Paul, L. Persson, S. Pilotte, D. C. Radford, H. Schnare, P. Vaska, D. Ward, J. N. Wilson, and I. Ragnarsson, Phys. Rev. C **50**, 484 (1994).

[6] H. Harada, M. Sugawara, H. Kusakari, H. Shinohara, Y. Ono, K. Furuno, T. Hosoda, M. Adachi, S. Matsuki, and N. Kawamura, Phys. Rev. C **39**, 132 (1989).

[7] M. Schimmer, S. Albers, A. Dewald, A. Gelberg, R. Wirowski, and P. von Brentano, Nucl. Phys. **A539**, 527 (1992).

[8] G. Ch. Madueme, L. Westerberg, L. O. Edvardson, and M. Migahed, Phys. Scr. **12**, 189 (1975).

[9] I. N. Vishnevsky, Yu. A. Dei, Yu. N. Lobach, I. P. Tkachuk, and V. V. Trishin, Izv. Akad. Nauk SSSR, Ser. Fiz. **52**, 168 (1988).

[10] I. N. Vishnevsky, Yu. N. Lobach, and V. V. Trishin, Izv. Akad. Nauk SSSR, Ser. Fiz. **55**, 2176 (1991).

[11] O. Hashimoto, Y. Shida, G. Ch. Madueme, H. Yoshikawa, M. Sakai, and S. Ohya, Nucl. Phys. **A318**, 145 (1979).

[12] J. Blachot and G. Marguier, Nucl. Data Sheets **67**, 1 (1992).

[13] J. M. Sears, D. B. Fossan, S. E. Gundel, I. Thorslund, P. Vaska, and K. Starosta, Phys. Rev. C **55**, 1096 (1997).

[14] A. Savelius, S. Juutinen, K. Helariutta, P. Jones, R. Julin, P. Jämsen, M. Muikku, M. Piiparinen, J. Suhonen, S. Törmänen,

R. Wyss, P. T. Greenlees, P. Simecek, and D. Cutoiu, Nucl. Phys. **A637**, 491 (1998).

[15] W. K. Dagenhart, P. H. Stelson, F. K. McGowan, R. L. Robinson, W. T. Milner, S. Raman, and W. K. Tuttle III, Nucl. Phys. **A284**, 484 (1977).

[16] I. Kh. Lemberg and A. A. Pasternak, *Modern Methods of Nuclear Spectroscopy* (Nauka, Leningrad, 1985).

[17] A. D. Efimov, M. F. Kudojarov, A. S. Li, A. A. Pasternak, I. Adam, M. Honusek, and A. Spalek, Yad. Fiz. **58**, 3 (1995) [Phys. At. Nucl. **58**, 1 (1995)].

[18] Yu. N. Lobach and D. Bucurescu, Phys. Rev. C **57**, 2880 (1998).

[19] Yu. N. Lobach and D. Bucurescu, Phys. Rev. C **58**, 1515 (1998).

[20] Yu. N. Lobach, A. A. Pasternak, J. Srebrny, Ch. Droste, G. B. Hagemann, S. Juutinen, T. Morek, M. Piiparinen, E. O. Podsvirova, S. Törmänen, K. Starosta, A. Virtanen, and A. A. Wasilewski, Acta Phys. Pol. B (to be published).

[21] J. Lindhard, V. Nielsen, and M. Scharff, K. Dan. Vidensk. Selsk. Mat. Fys. Medd. **36**, 10 (1968).

[22] I. Kh. Lemberg and A. A. Pasternak, Nucl. Instrum. Methods **140**, 71 (1977).

[23] R. Schwengner, G. Winter, J. Döring, L. Funke, P. Kemnitz, E. Will, A. E. Sobov, A. D. Efimov, M. F. Kudojarov, I. Kh. Lemberg, A. S. Mishin, A. A. Pasternak, L. A. Rassadin, and I. N. Chugunov, Z. Phys. A **326**, 287 (1987).

[24] J. Urbon, D. G. Sarantites, and L. L. Rutledge, Nucl. Instrum. Methods **126**, 49 (1975).

[25] H. P. Hellmeister, K. P. Lieb, and W. Muller, Nucl. Phys. **A307**, 515 (1978).

[26] W. F. Van Gunsteren, K. Allaart, and P. Hofstra, Z. Phys. A **228**, 49 (1978).

[27] F. Andreozzi, L. Coraggio, A. Covello, A. Gargano, and A. Porrino, Z. Phys. A **354**, 253 (1996).

[28] A. Insolia, N. Sandulescu, J. Blomquist, and R. J. Liotta, Nucl. Phys. **A550**, 34 (1992).

[29] G. Momoki, K. Ogawa, and I. Tohozuka, University of Tokyo, INS Report 1985, p. 563.

[30] A. K. Singh, G. Gangopadhyay, and D. Banerjee, Phys. Rev. C **53**, 2524 (1996).

[31] A. I. Vdovin, Ch. Stoyanov, and W. Andrejtscheff, Nucl. Phys. **A440**, 437 (1985).

[32] J. Toivanen and J. Suhonen, J. Phys. G **21**, 1491 (1995); Phys. Rev. C (submitted).

[33] E. J. Schneid, A. Prakash, and B. L. Cohen, Phys. Rev. **156**, 1316 (1967).

[34] P. H. Stelson, W. T. Milner, F. K. McGowan, R. L. Robinson, and S. Raman, Nucl. Phys. **A190**, 197 (1972).

[35] H. Prade, W. Enghardt, W. D. Fromm, H. U. Jäger, L. Käubler, H. J. Keller, L. K. Kostov, F. Stary, G. Winkler, and L. Westerberg, Nucl. Phys. **A425**, 317 (1984).

[36] A. De-Shalit, Phys. Rev. **122**, 1530 (1961).

[37] I. N. Vishnevsky, G. B. Krygin, Yu. N. Lobach, V. E. Mitroshin, A. A. Pasternak, and V. V. Trishin, Ukr. Fiz. Zh. **36**, 1132 (1991).